inotiv
analyze. answer. advance.

White paper

Development, Characterization, and Validation of B-NDG hIL15 Mice

A Novel Mouse Strain Expressing Human IL15 on an Ultra-Immunodeficient B-NDG Background

inotivco.com

Contents

The NOD.CB17-*Prkdc*^{scid} *IL2rg*^{tm1}/BcgenHsd (B-NDG) knockout mouse is a highly immunodeficient model that is a new alternative option among the ultra-immunodeficient category of models.

The B-NDG mouse has recently become commercially available from Envigo, and it was originally developed by Biocytogen, and Envigo acquired it from Biocytogen in 2019. This powerful model lacks mature B cells, T cells, and natural killer (NK) cells and is cytokine signaling pathways are blocked for six different interleukins (IL-2, IL-4, IL-7, IL-9, IL-15, and IL-21). It is suitable for engraftment with human cancer cells or tissue, including for patient-derived xenograft (PDX) tumor models and humanized models with CD34+ human hematopoietic stem cells (HSCs) or peripheral blood mononuclear cells (PBMCs).

While the B-NDG model is invaluable for many types of *in vivo* studies, a recognized limitation has been that B-NDG mice engrafted with a human immune system lack functional NK cells and therefore are not ideal for studies targeting those cells.

To overcome this limitation, a novel mouse strain has been developed on the B-NDG background. This new strain, known as "B-NDG hIL15" [NOD.CB17-*Prkdc*^{scid}*Il2rg*^{tm1}*Il15*$^{tm1(IL15)}$/BcgenHsd], was generated to express the human IL15 cytokine, which is essential to properly establish NK cells (Lin *et al*., 2020; Wu *et al*., 2017). Expression of hIL15 boosts the development and survival of functional human NK cells in the context of immunodeficient mice engrafted with human cells; this is an especially valuable tool for evaluating NK cell-based immunotherapies and their function in tumorigenesis.

This white paper reviews the development and characterization of the B-NDG hIL15 mouse, including its suitability for developing cell-line-derived xenograft (CDX) and PDX models and studying therapeutic agents that benefit from long-term maintenance of human NK cells. The B-NDG hIL15 model was developed by Biocytogen and Envigo licensed this strain from Biocytogen in 2021 and currently maintains and distributes it.

Introduction

NK cells are a highly relevant target for immunotherapy because they possess an innate ability to detect and kill cancer cells (Wu *et al.*, 2020; Meza Guzman *et al.*, 2020). While humanized mice in strains such as B-NDG are powerful models for studying immunotherapies that activate T cells, they are not ideal for those targeting NK cells, since human NK cells do not sufficiently develop and function in these animals.

IL-15 encodes a cytokine that plays an important role in immune cell development; NK cells were shown to be virtually nonexistent in IL15$^{-/-}$ mice (Kennedy *et al.*, 2000), and mature NK cells fail to be maintained when transferred to IL-15$^{-/-}$ mice (Cooper *et al.*, 2002), which supports IL15's critical role in NK cell differentiation and survival (Figure 1).

Figure 1: IL-15 is critical for the differentiation of mature NK cells from NK cell precursors. NK cell development from hematopoietic stem cells (HSCs) is regulated by multiple cytokines. IL-15 is indispensable for NK cell differentiation to mature NK cells. Note: iNK (immature NK cells); mNK (mature NK cells), NKP (NK lineage-restricted progenitors), CLP (common lymphoid progenitors). Image and figure legend text (edited) from Wu *et al.* (2017). *Developmental and Functional Control of Natural Killer Cells by Cytokines. Frontiers in Immunology. 04 August 2017; doi.org/10.3389/fimmu.2017.00930. Used under Creative Commons Attribution (CC BY) license (https://creativecommons.org/licenses/by/4.0/).*

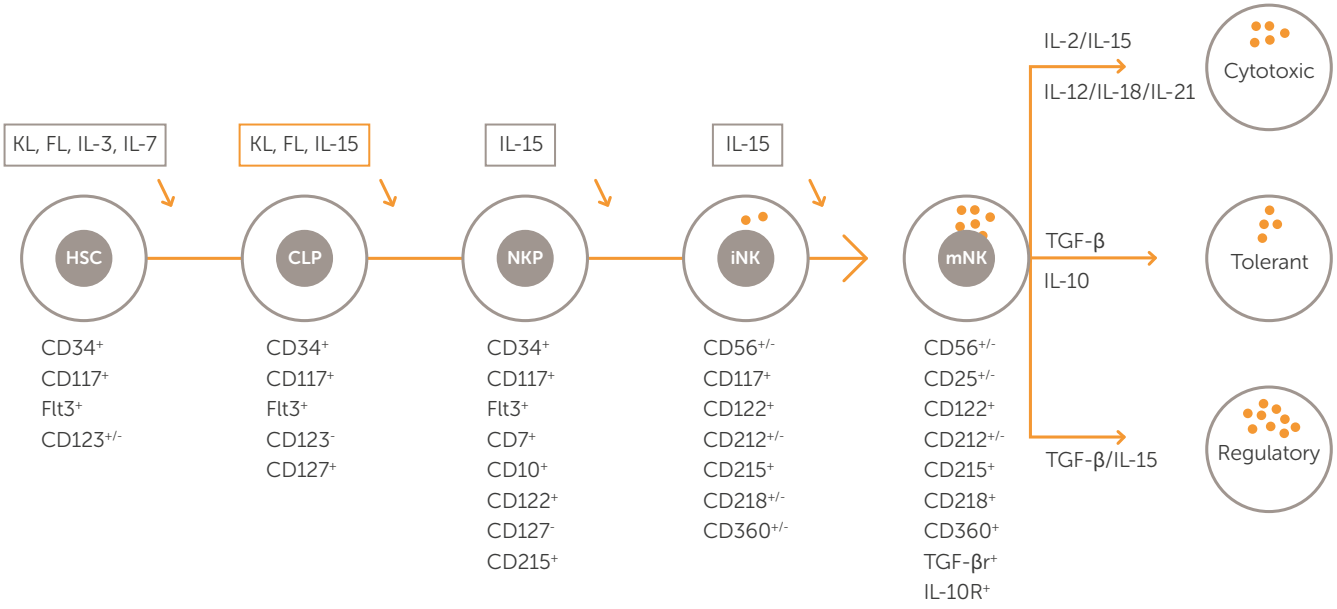

The B-NDG hIL15 [NOD.CB17-*Prkdc*^{scid}*Il2rg*^{tm1}*Il15*^{tm1}/BcgenHsd] strain was designed to overcome this deficiency (after engraftment with a human immune cells) by expressing the human IL15 cytokine (Lin *et al.*, 2020; Wu *et al.*, 2017).

As described in detail below, B-NDG hIL15 mice can be successfully engrafted with a human immune system (PBMCs and HSCs) that develops functional human NK cells. This model allows researchers to study novel immunotherapies targeting NK cells in mice with a B-NDG background.

Generation of the B-NDG hIL15 Mouse

The B-NDG hIL15 model is a knockout mouse with an ultra-immunodeficient phenotype, which combines a B-NDG mouse background that expresses the human *IL15* cytokine.

It was generated by first deleting the *IL2rg* gene from NOD-scid mice. The *Prkdc* (protein kinase DNA-activated catalytic) null scid mutation is characterized by a significant deficiency in functional T cells and B cells.

The common gamma chain gene (IL2RG) deletion results in a lack of functional receptors for IL-2, IL-4, IL-7, IL-9, IL-15, and IL-21, producing a lack of functional NK cells.

The coding sequence region of the human *IL15* gene was inserted after the 5'UTR of the mouse Il15 (Figure 2). This strain was then confirmed to express the human *IL15* cytokine (Figure 3).

Figure 2: Schematic showing insertion of hIL15 gene at the mouse 5'UTR locus.

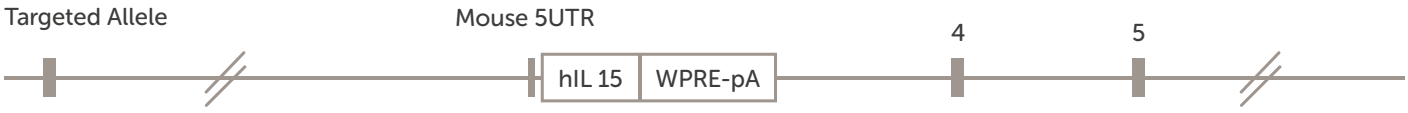

Figure 3: Strain specific mRNA and protein analysis of IL15 in B-NDG and B-NDG hIL15 mice. (A) RT-PCR results show mouse IL15 (mIL15) mRNA was detectable only in splenocytes of B-NDG mice (+/+), while human IL15 mRNA was detectable only in homozygous B-NDG hIL15 (H/H). (B) ELISA results from serum samples of animals stimulated with poly(I:C) confirm that human IL15 is detectable in homozygous B-NDG hIL15 (H/H) mice but not in B-NDG (+/+) mice.

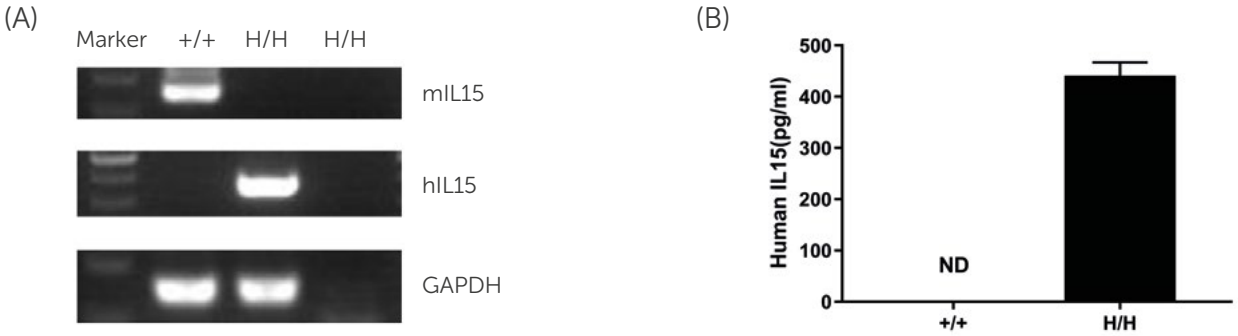

THE FOLLOWING SECTIONS PROVIDE PHENOTYPIC, PHARMACOKINETIC, AND EFFICACY ASSESSMENTS FOR THIS NOVEL MOUSE STRAIN:

- Human immune system engraftment with HSCs, including the development of five CDX models (using a variety of cell lines, including K562, MV-4-11, Panc-1, Raji-luc, and A549-hCLDN18.2) and a pancreatic PDX model, in addition to antitumor efficacy studies in a subset of these models;
- Human immune system engraftment with PBMCs, including the development of two CDX models and efficacy assessments in these models; and
- Data from human NK cell reconstitution and efficacy assessment in a CDX model

Human Immune System Engraftment with HSCs

IMMUNE CELL PHENOTYPING

Human immune cell phenotyping was conducted in B-NDG hIL15 mice engrafted with human HSCs. After myeloablation (1.6 Gy irradiation), human CD34+ cells were intravenously injected into homozygote female B-NDG hIL15 (6 weeks old, n=19) and B-NDG (6 weeks old, n=17) mice. Representative flow cytometric analyses of peripheral blood lymphocytes demonstrate that B-NDG hIL15 mice have a higher percentage of human NK cells as compared with B-NDG mice, and these data confirm the presence of human T cells and B cells in reconstituted B-NDG hIL15 mice (Figure 4).

Figure 4: Flow cytometry data evaluating levels of human immune cells in both B-NDG and B-NDG hIL15 mice.

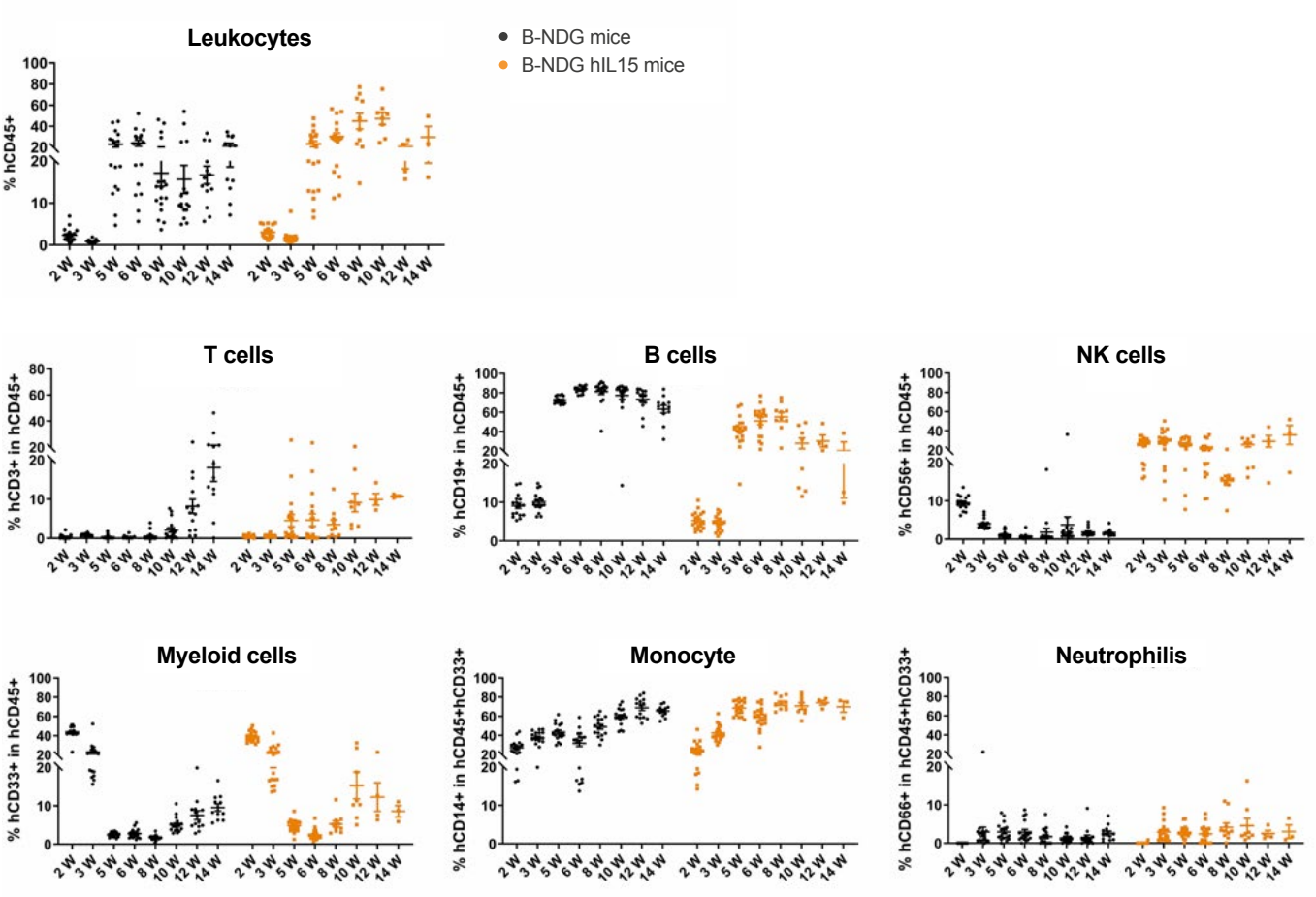

CDX MODEL DEVELOPMENT

After myeloablation, human CD34+ cells were engrafted intravenously into a cohort of homozygous female B-NDG hIL15 (7 weeks old, n=30) and B-NDG control mice. Animals were considered sufficiently humanized if they exhibited ≥10% hCD45+ cells in the blood. Animals received subcutaneous injections of one of the following cancer cell lines to establish the CDX models:

- K562 (lymphoblast line derived from a patient with chronic myelogenous leukemia),
- MV-4-11 (macrophage line derived from a patient with biphenotypic B myelomonocytic leukemia), or
- Panc-1 (pancreatic cancer).

Tumor volumes were measured in these CDX models a period of 5 weeks post-engraftment with HSCs. As shown in Figure 5, all three cell lines formed tumors in both cohorts of mice, but tumors in the B-NDG hIL15 mice exhibited significantly delayed development as compared to the control B-NDG animals.

Figure 5: Tumor volumes in CDX models developed in humanized B-NDG and B-NDG hIL15 mice using (A) K562, (B) MV-4-11, and (C) Panc-1 cell lines.

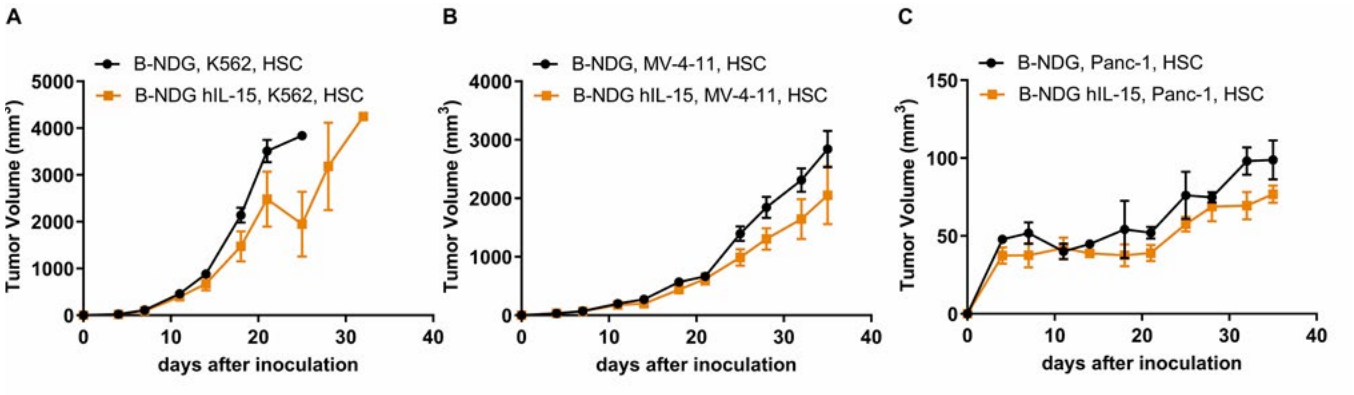

During the 5 weeks following HSC engraftment, levels of human leukocytes (hCD45+), T cells (%hCD3+ in the hCD45+ population), and NK cells (%hCD56+ in the hCD45+ population) were measured in peripheral blood in both strains of mice. As shown in Figure 6, each of the three CDXs in B-NDG hIL15 mice had significantly higher levels of the measured human immune cells as compared to their B-NDG counterparts.

Figure 6: Levels of human immune cells in B-NDG and B-NDG hIL15 mice implanted with (Top panel) K562, (Middle panel) MV-4-11, and (Bottom panel) Panc-1 cell lines.

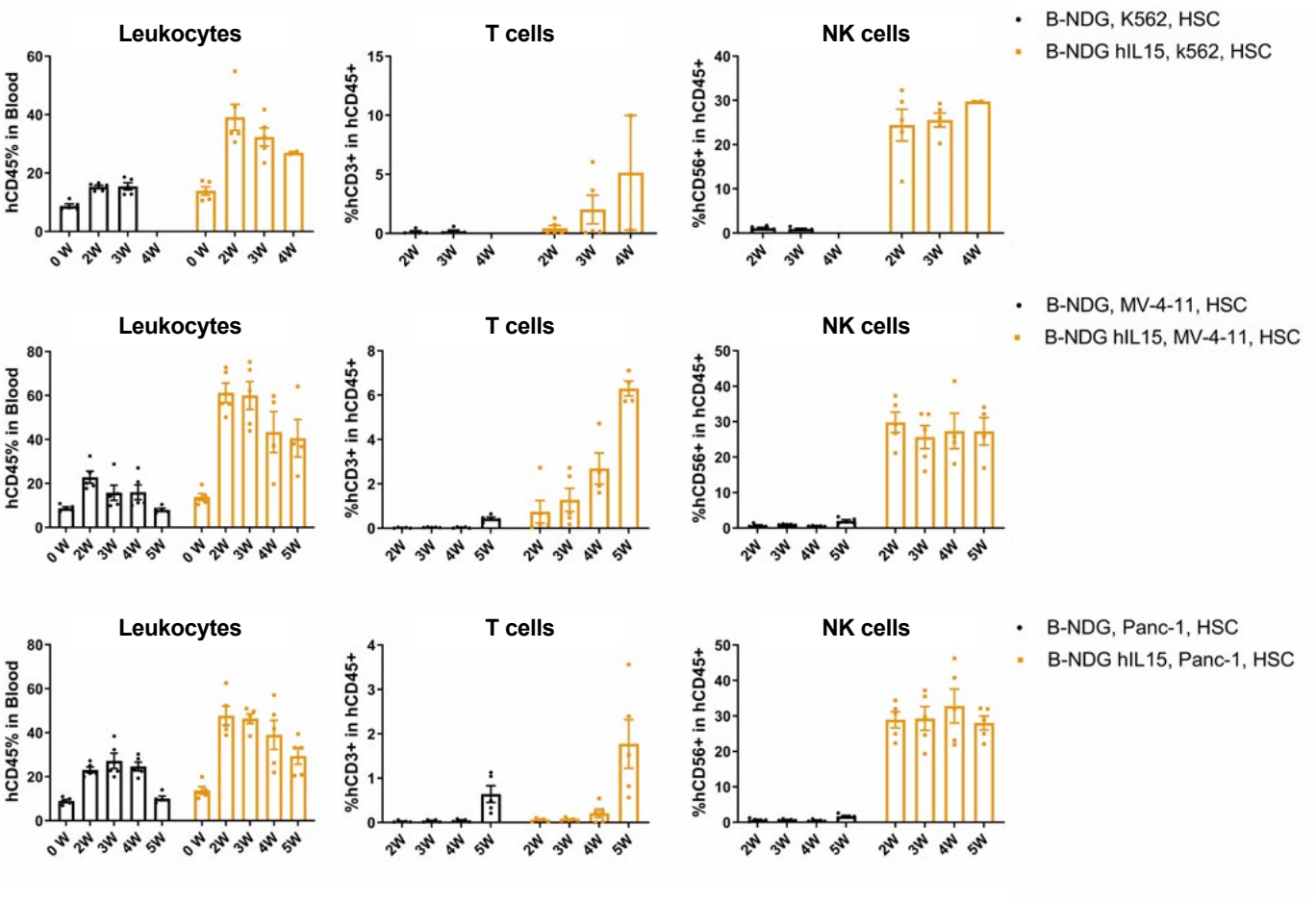

A detailed analysis of the MV-4-11 and Panc-1 CDX model shows that blood and tumor tissues in the B-NDG hIL15 mice have a higher percentage of human NK cells as compared with the B-NDG mice, and the NK cells express functional proteins (measured via Granzyme B and Perforin levels) (Figure 7).

Figure 7: Proportion and function of NK cells in blood and tumor tissue from B-NDG hIL15 and B-NDG mice humanized with HSCs and implanted with (A) MV-4-11, and (B) Panc-1 cells.

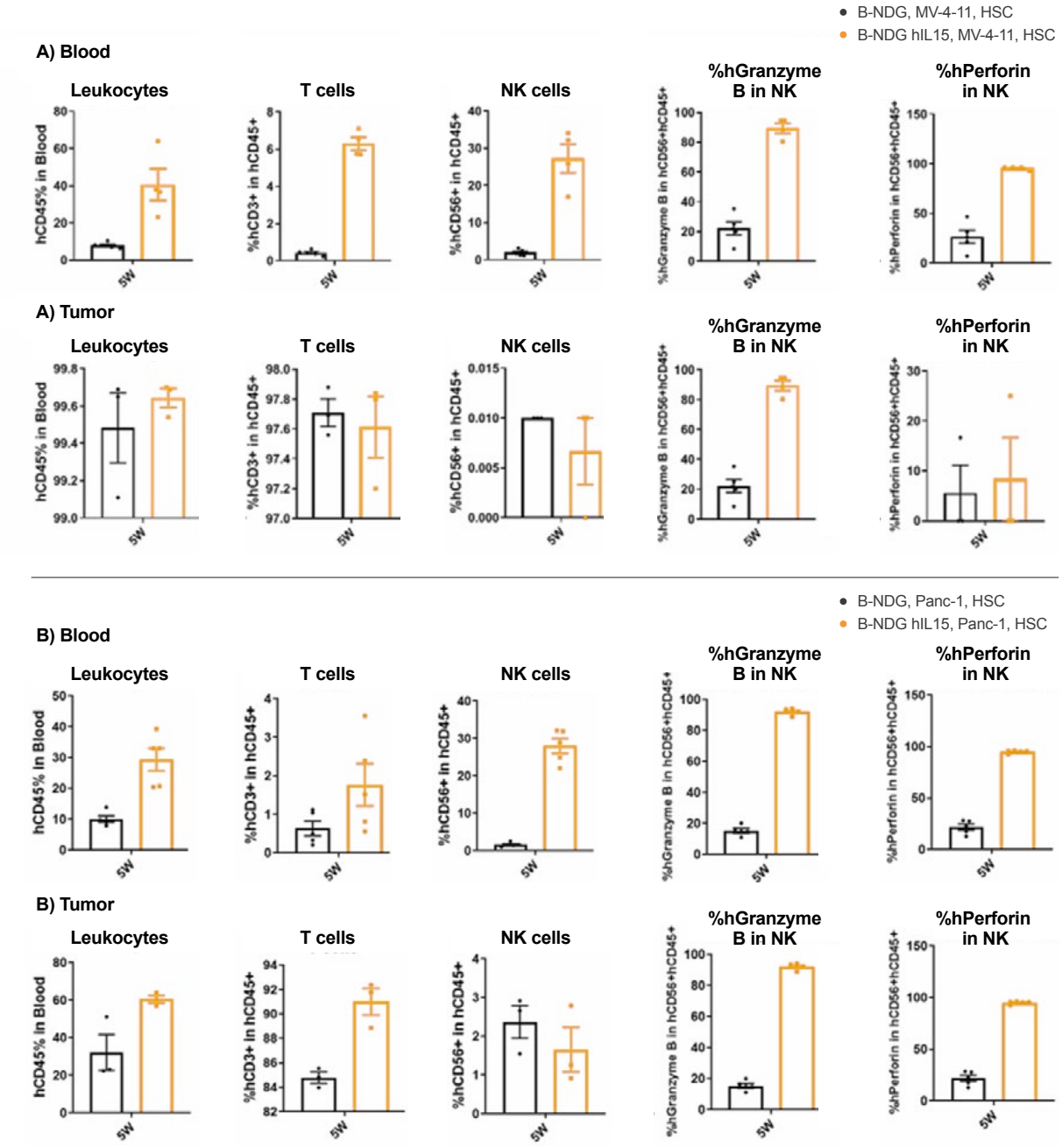

CDX Model Development and Anti-Tumor Drug Efficacy Testing

RAJI-LUC MODEL

A fourth CDX model was developed using Raji-Luc cells. Tumor development was monitored using fluorescence imaging (Figure 8A), and body weight (Figure 8B) and survival rates (Figure 8C) were also evaluated over the 40-day study period. Raji-Luc cells successfully formed tumors in both cohorts, and tumor growth was delayed in the B-NDG hIL15 mice compared to the control B-NDG animals (Figure 8).

Figure 8: (A) Tumor growth as per immunofluorescence imaging intensity, (B) body weights, and (C) survival rates of B-NDG and B-NDG hIL15 mice humanized with HSCs and implanted with Raji-luc cells.

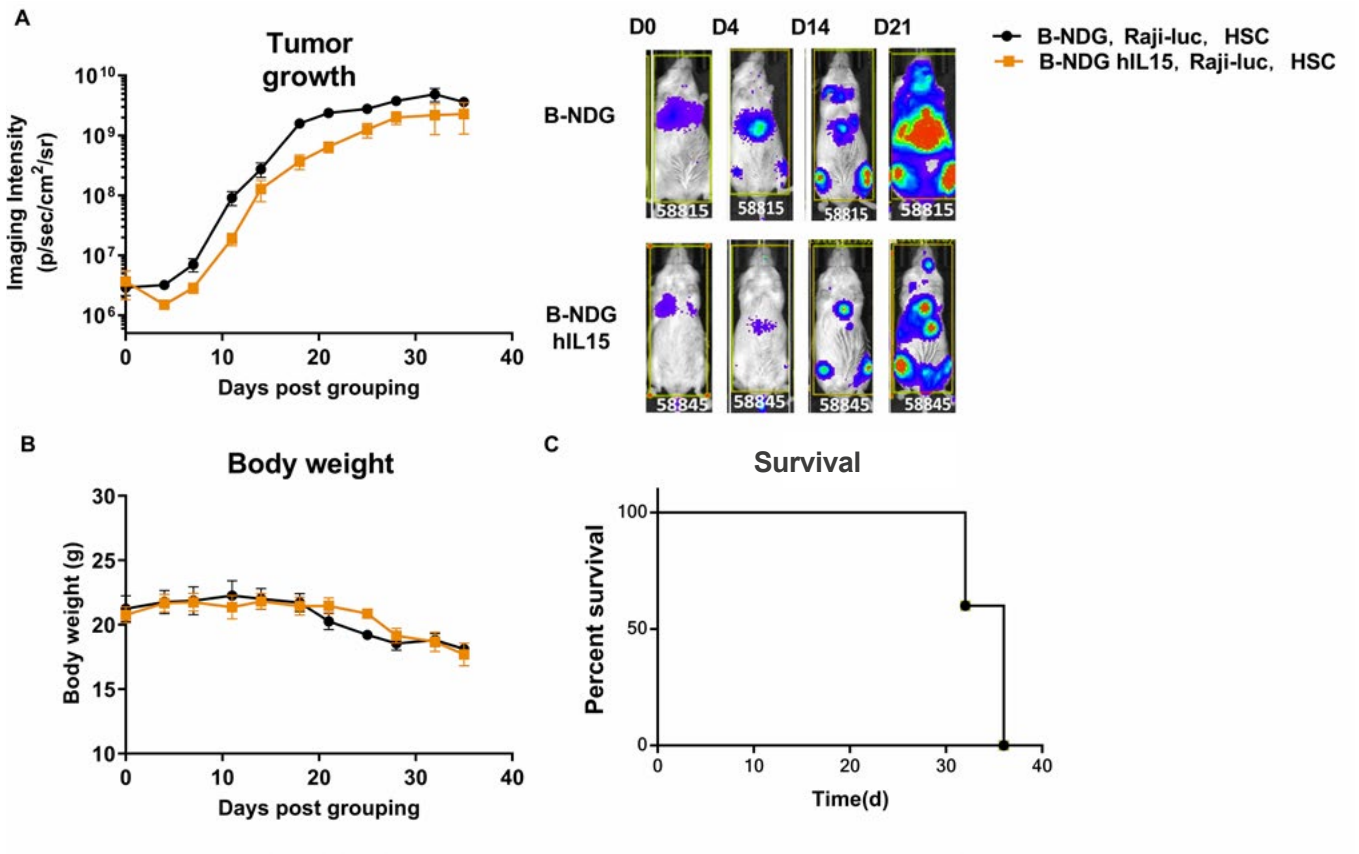

The efficacy of an anti-human CD20 antibody (rituximab) against Raji-luc cells was then assessed in the B-NDG hIL15 animals as compared to untreated control animals. Rituximab is believed to bind and polarize B cells, a mechanism that is thought to enhance its therapeutic function by triggering NK-cell mediated antibody dependent cellular cytotoxicity (ADCC) (Rudnicka *et al.*, 2013). Tumor volumes were allowed to reach 100-150mm^3 (n=5) before initiating treatment that was dosed at 100µg rituximab per mouse every three days.

Figure 9: (A) Raji-luc growth in rituximab treated and untreated B-NDG hIL15 mice, (B) Data from individual animals in rituximab treated and untreated animals, and (C) Leukocyte and NK cell counts in rituximab treated B-NDG hIL15 mice implanted with Raji-luc cells.

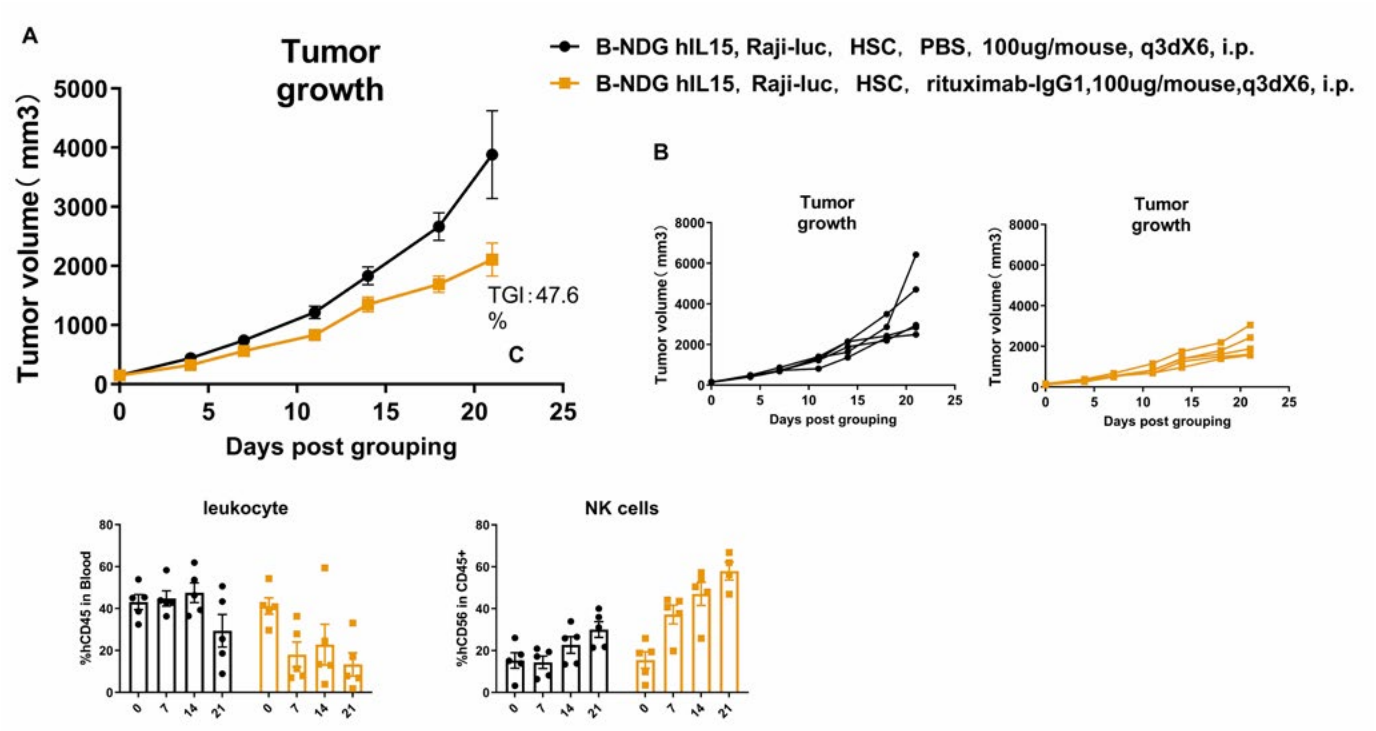

A549-HCLDN18.2 MODEL

A fifth CDX model was generated in B-NDG hIL15 mice by implanting them with A549-hCLDN18.2 cells to evaluate the efficacy of IMAB362, an experimental monoclonal antibody targeting isoform 2 of human Claudin-18 (i.e., Claudin-18.2). IMAB362 was administered twice weekly at a dose of 25mg/kg beginning when the tumor size reached approximately 50mm^3 (n=5). TGI for IMAB362 was found to be 28.5% (Figure 10A) and the IMAB362-treated animals maintained a body weight that was similar to the untreated control animals (Figure 10B).

Figure 10: (A) Tumor growth and (B) body weight of B-NDG hIL15 mice implanted with A549-hCLDN18.2 cells and treated or not with anti-human Claudin 18.2 antibody.

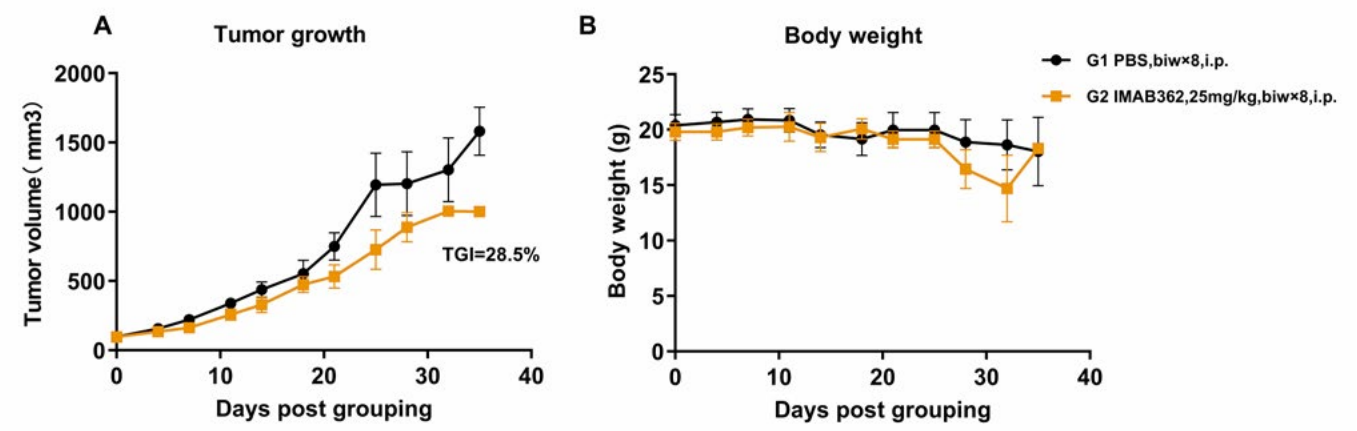

PDX Model Development and Anti-Tumor Drug Efficacy Testing

Human CD34+ HSC-engrafted B-NDG hIL15 mice were used to generate a pancreatic cancer PDX model that was used to test the efficacy of cetuximab (Erbitux), an epidermal growth factor receptor (EGFR) inhibitor. Once weekly treatments of 40mg/kg were initiated when tumor volumes reached approximately 100mm^3 (n=5). As shown in Figures 11A and 11B, a TGI of 35.1% was achieved for cetuximab, with robust levels of leukocytes and NK cells demonstrated over the treatment period (Figure 11C).

Figure 11: A) PDX growth in cetuximab treated and untreated B-NDG hIL15 mice, (B) Data from individual animals in cetuximab treated and untreated animals, and (C) Leukocyte and NK cell counts in cetuximab treated pancreatic cancer PDX established in B-NDG hIL15 mice.

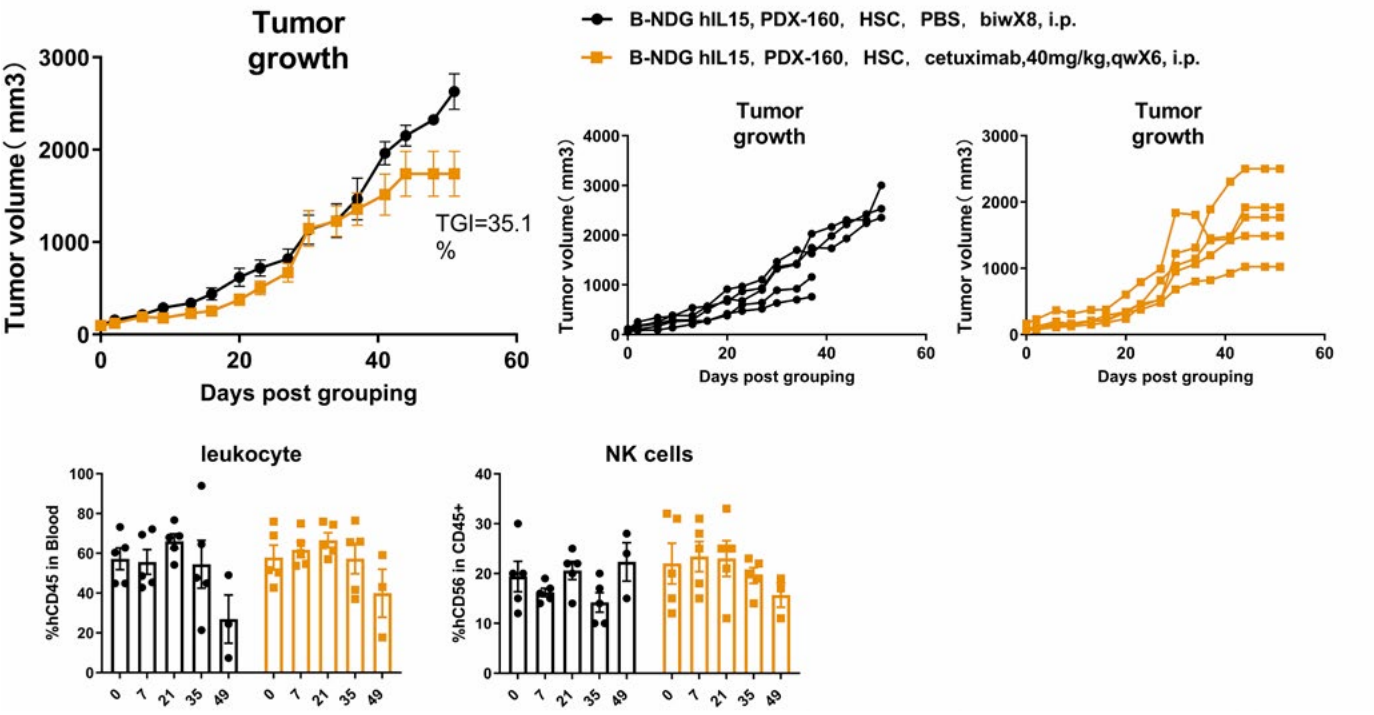

[1] *A549-hCLDN18.2 cells have the human CLDN18.2 coding sequence inserted into the AAVS1 locus in A549 cells. Human CLDN18.2 is highly expressed on the surface of B-hCLDN18.2 A549 cell*

Human Immune System Engraftment with PBMCs

IMMUNE CELL PHENOTYPING

Human immune cell phenotyping was conducted in B-NDG hIL15 mice engrafted with $5x10^6$ human PBMCs which were intravenously injected into female B-NDG hIL15 (n=15) and B-NDG (n=10) mice at 5 weeks of age.

Human immune cell phenotyping was conducted at different time points over the 6-week study period. Cell types were assessed via flow cytometry and included leukocytes, T cells, CD4+ and CD8+ T cells, NK cells, and Treg cells. Survival and body weight were also measured over the duration of the study. Results demonstrate that human NK cells and T cells were successfully propagated in both the B-NDG and B-NDG hIL15 mice, albeit B-NDG hIL15 mice were clearly superior with respect to NK cell counts (Figure 12A and 12B). Furthermore, the propagated NK cells were found to express NK functional proteins (human Granzyme B and human Perforin) (Figure 12B). Similar survival rates were seen for both cohorts of animals (Figure 12C), and body weights were higher for B-NDG animals during the course of the study (Figure 12D). These data suggest that human NK and T cells in reconstituted B-NDG IL15 mice are successfully propagated.

Figure 12: (A) Successful propagation of human T cells and NK cells in B-NDG and B-NDG hIL15 mice humanized via PBMC engraftment, and (B) propagated NK cells are functional in PBMC-engrafted B-NDG hIL15 mice. (C) Percent survival, and (D) Body weight of B-NDG hIL15 and B-NDG mice humanized with PBMCs. Results expressed as mean ± SEM.

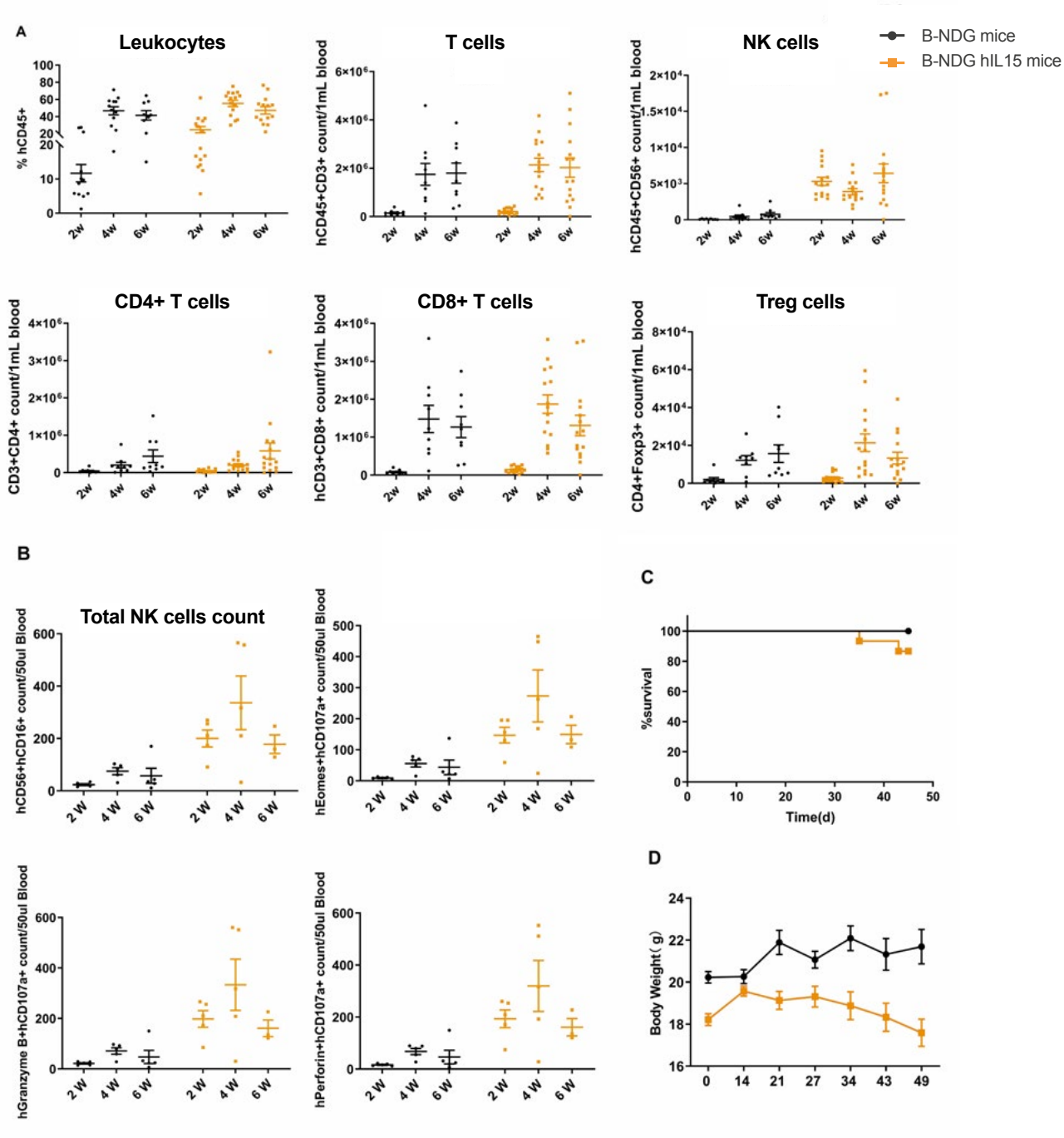

CDX Model Development

Human PBMC-engrafted B-NDG hIL15 (n=5) and B-NDG (n=5) mice were used to establish a CDX model using K562 cells. Six-week-old female mice received an intravenous injection of $5x10^6$ PBMCs and subcutaneous implantation of K562 ($1x10^6$) cells on the same day. Tumor volume and body weight were measured throughout the study period, as were levels of human leukocytes and NK cells.

Tumor growth in B-NDG hIL15 mice was significantly delayed, with some reduction in body weight beginning after approximately 1 week, albeit this was no longer statistically significant after 2 weeks (Figure 13). B-NDG hIL15 mice also showed a higher percentage of human CD45+ cells and higher cell numbers of human NK cells as compared to B-NDG control animals at the 2- and 3-week time points.

Figure 13: Tumor volume, body weight, and flow cytometry analyses of human leukocytes and NK cells in PBMC-engrafted B-NDG hIL15 and B-NDG mice implanted with K562 cells. Results expressed as mean ± SEM.

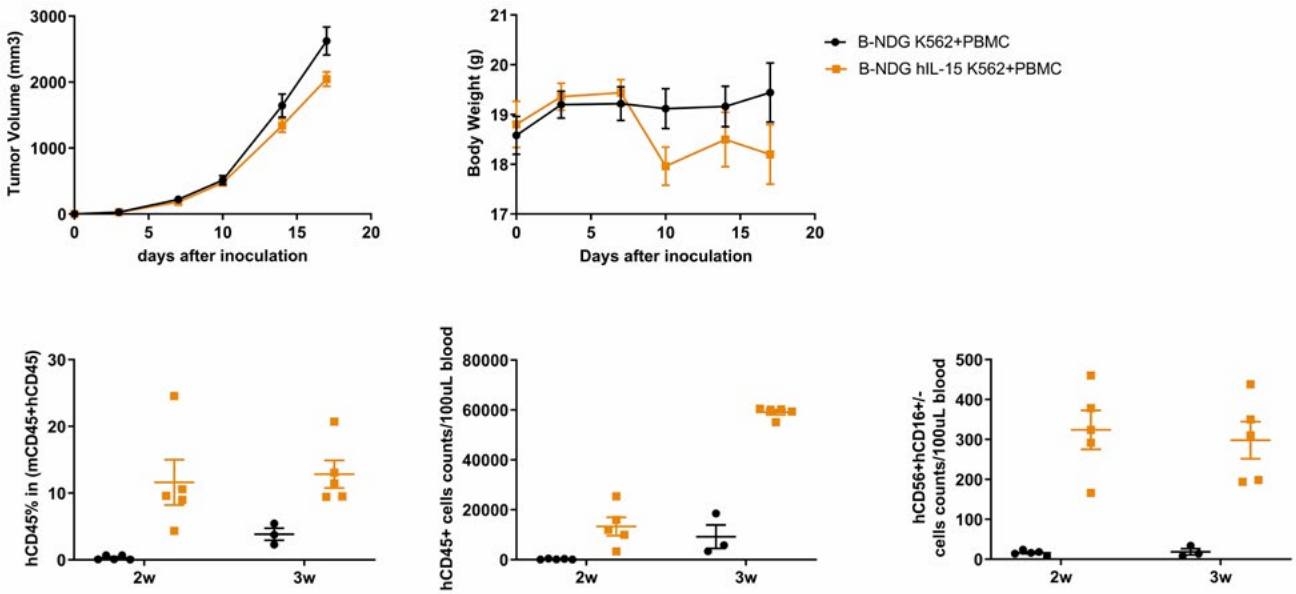

A second CDX model using Panc-1 cells was similarly developed in human PBMC-engrafted B-NDG hIL15 (n=5) and B-NDG (n=5) mice. Six-week-old female mice received an intravenous injection of $5x10^6$ PBMCs and subcutaneous implantation of Panc-1 ($5x10^6$) cells on the same day. Tumor volume and body weight were measured throughout the study period, as were levels of human leukocytes and NK cells.

Figure 14 shows that tumor growth and body weight of B-NDG hIL15 mice was significantly delayed and reduced, respectively. B-NDG hIL15 mice also showed an increase in the percentage of human CD45+ cells and an increase in the cell number of human NK cells.

Figure 14: Tumor volume, body weight, and flow cytometry analyses of human leukocytes and NK cells in PBMC-engrafted B-NDG hIL15 and B-NDG mice implanted with Panc-1 cells. Results expressed as mean ± SEM.

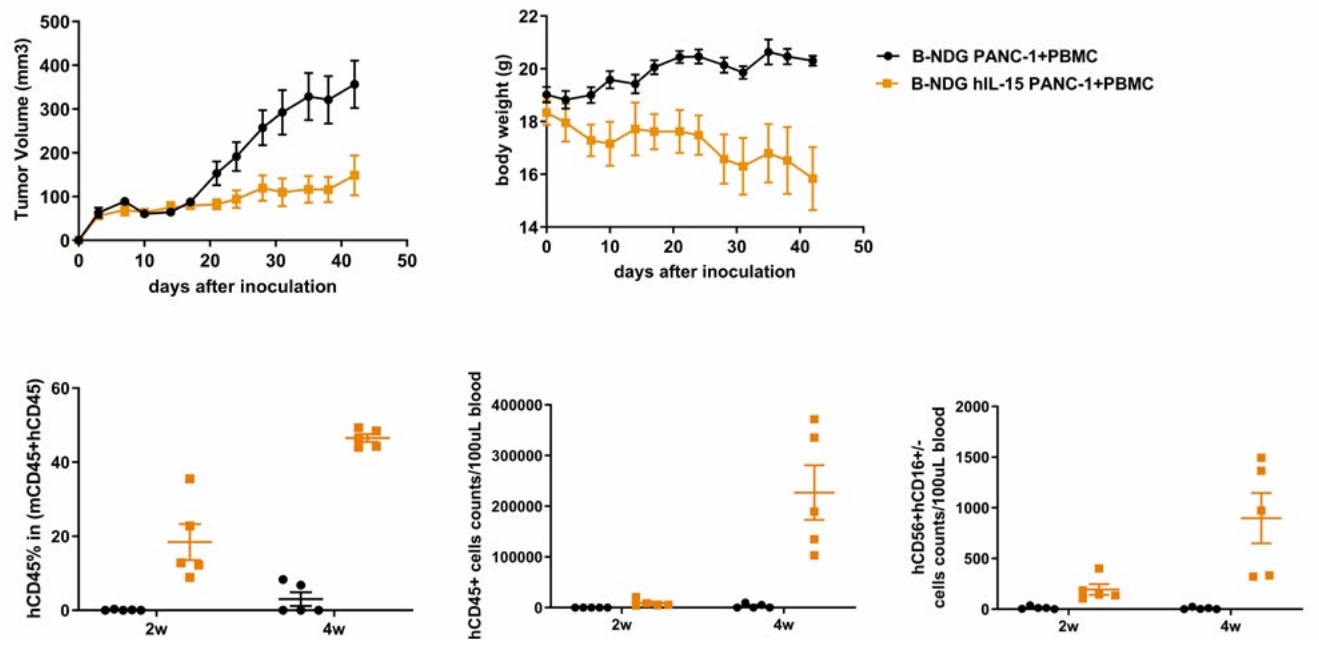

CDX Model Development and Anti-Tumor Drug Efficacy Testing

A third CDX model was generated to test the efficacy of the IMAB362 monoclonal antibody described earlier (i.e., targeting human Claudin 18.2). To do this, $6x10^6$ NUGC4-CLDN18.2 cells were subcutaneously implanted into human PBMC-engrafted ($1x10^6$ PBMCs) B-NDG hIL15 mice.

Once tumors reached 70-100mm^3 (n=5), mice were treated with IMAB362 (10mg/kg) twice weekly for a period of ~3 weeks. As shown in Figure 15, a TGI of 30.9% was achieved for IMAB362, with body weights of these animals closely paralleling those of the untreated control animals.

Figure 15: (A) IMAB362 significantly delayed tumor growth of NUGC4-CLDN18.2 cells in B-NDG hIL15 mice, and (B) Body weights were similar throughout the study period for the IMAB362-treated and untreated animals.

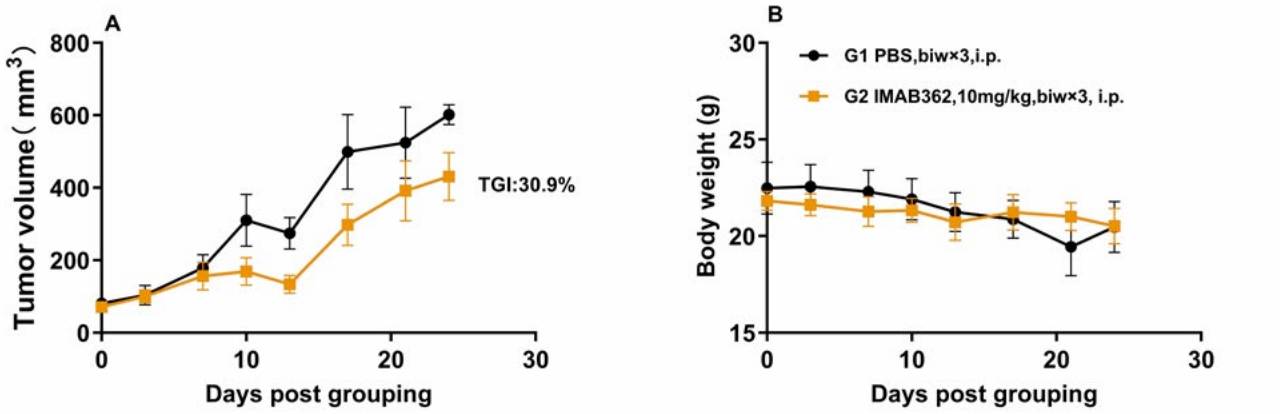

A fourth CDX model was generated to test the efficacy of Tiragolumab, a monoclonal antibody that targets TIGIT, an inhibitory checkpoint protein receptor that is expressed on multiple immune cell types, including NK and T cells (Solomon *et al*., 2018). To do this, a human melanoma cell line, A375, was subcutaneously implanted into human PBMC-engrafted B-NDG hIL15 mice. Twice weekly dosing at 8mg/kg Tiragolumab was initiated the day after animals were inoculated with tumor cells and continued for ~3 weeks.

As shown in Figure 16, a TGI of 29.1% was achieved for IMAB362, with body weights of these animals closely paralleling those of the untreated control animals.

Figure 16: (A) Tiragolumab delayed tumor growth of A375 cells in B-NDG hIL15 mice, and (B) Body weights were similar throughout the study period for the Tiragolumab treated and untreated animals.

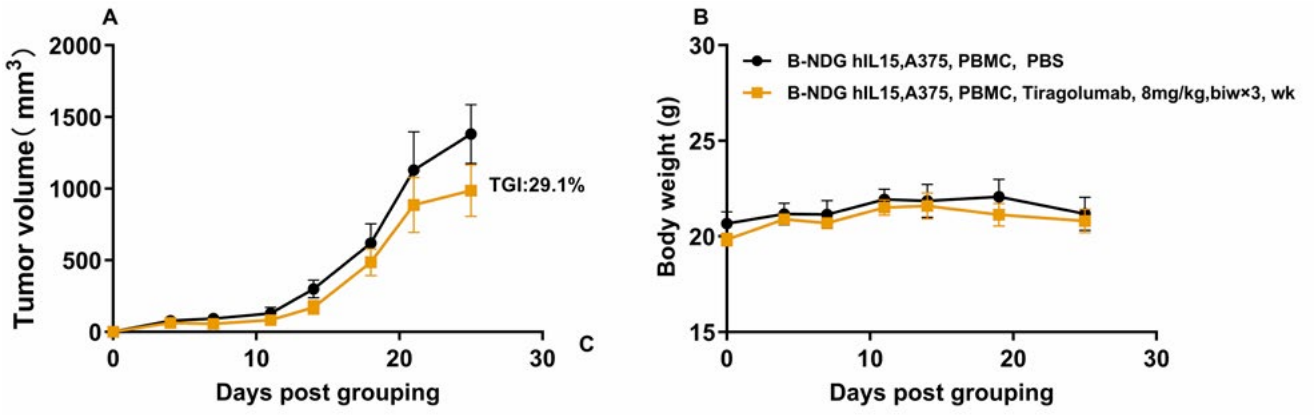

Human NK Cell Reconstitution

NK CELL VIABILITY AND PROPAGATION

Human NK cells were purified from human PBMCs, and 2 x 10^6 cells were intravenously injected into female 6-week-old B-NDG hIL15 (n=8) and B-NDG mice (n=8). Table 1 shows the changes in various immune cells during the different NK cell screening stages. Representative flow cytometry data from peripheral blood lymphocytes are shown in Figure 17. These count and percentage data demonstrate that B-NDG hIL15 animals outperformed B-NDG mice for supporting the viability and propagation of human NK cells over the 6-week study period.

PROPORTION OF EACH CELL	hCD45 (%)	hCD3 in hCD45 (%)	hD56 in hCD45 (%)	hD56 in hCD45 (%)	hD56 in hCD45 (%)
PBMC	99.89	72.33	7.44	--	1.13
after the kit sorted	99.96	1.31	80	73.35	17.89
14 days post injection	8.04	0.21	85.03	76.32	13.94

Figure 17: Flow cytometry analysis (count and percentage) of human NK cells in B-NDG hIL15 and B-NDG mice.

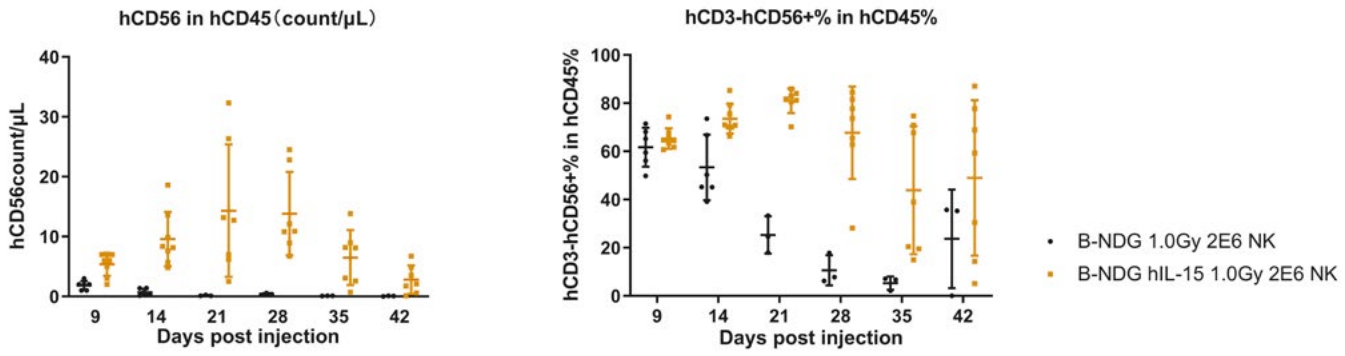

NK Cell Functionality

Several human NK cell functional markers were used to determine whether reconstituted NK cells were functional. Biomarkers included hGranzyme B, hNKG2A, hNKG2D, and hNKp46. The results of this analysis demonstrate that after reconstitution of NK cells, the levels of functional markers were significantly increased, indicating that the NK cells retain their killing ability (Figure 18). Other functional NK markers, including perforin, CD107, NKp30, and CD57 were shown to have similar trends (data not shown).

Figure 18: Flow cytometry results of functional NK cell biomarkers in in B-NDG hIL15 and B-NDG mice.

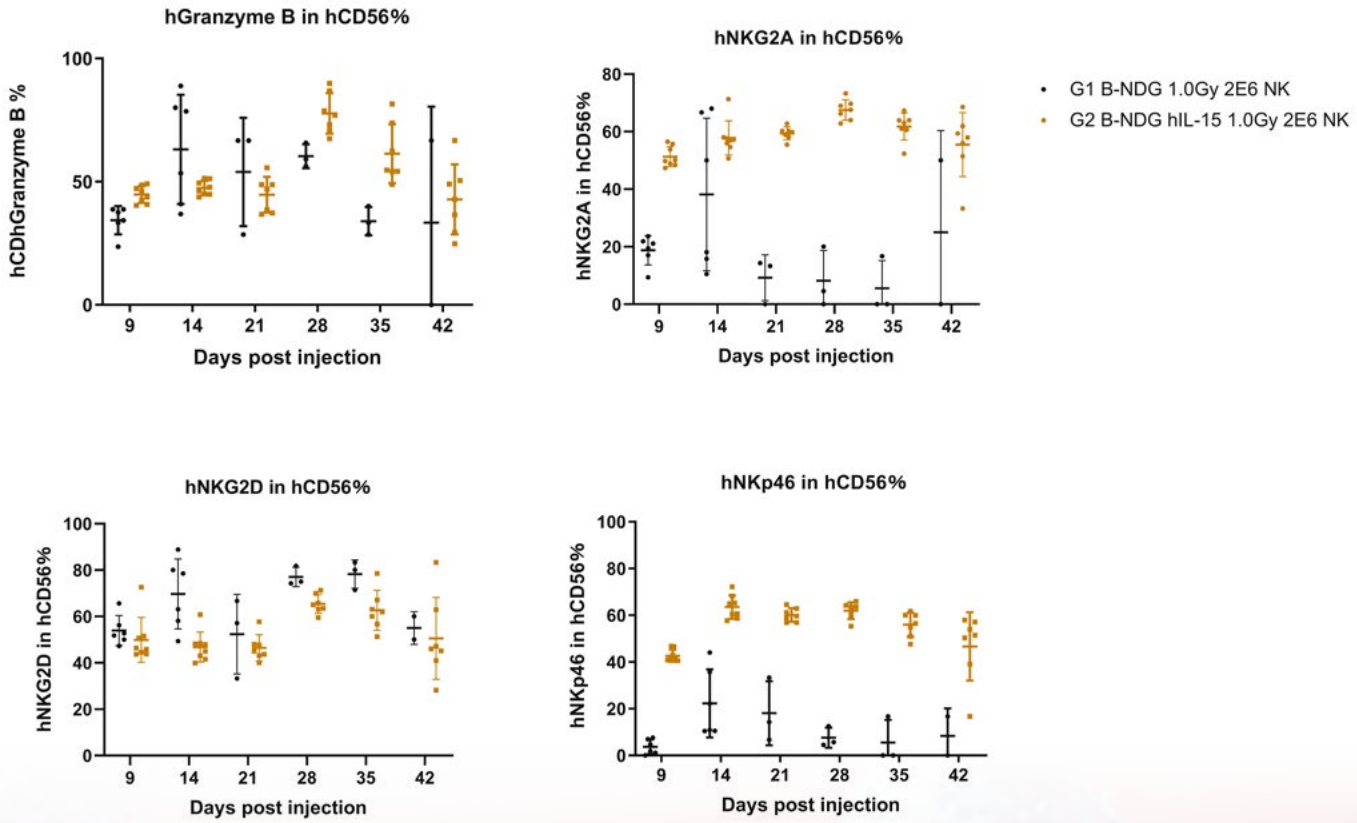

CDX Model Development and Anti-Tumor Drug Efficacy Testing

B-NDG hIL15 mice engrafted with human NK cells (2 x 10^6) were used to establish a CDX model using A549-hCLDN18.2 cells (1 x 10^7) for efficacy testing of IMAB362 (a monoclonal antibody targeting human Claudin 18.2 as described earlier). When tumors reached between 100-150mm^3 (n=6), mice were treated with IMAB362 at a dose of 10mg/kg twice weekly for a period of ~4 weeks.

Figure 19 shows that a TGI of 34% was achieved for IMAB362, with body weights of these animals closely paralleling those of the untreated control animals.

Figure 19: (A) Tumor growth, and (B) Body weights of B-NDG hIL15 mice implanted with A549-hCLDN18.2 cells and treated or not with IMAB362.

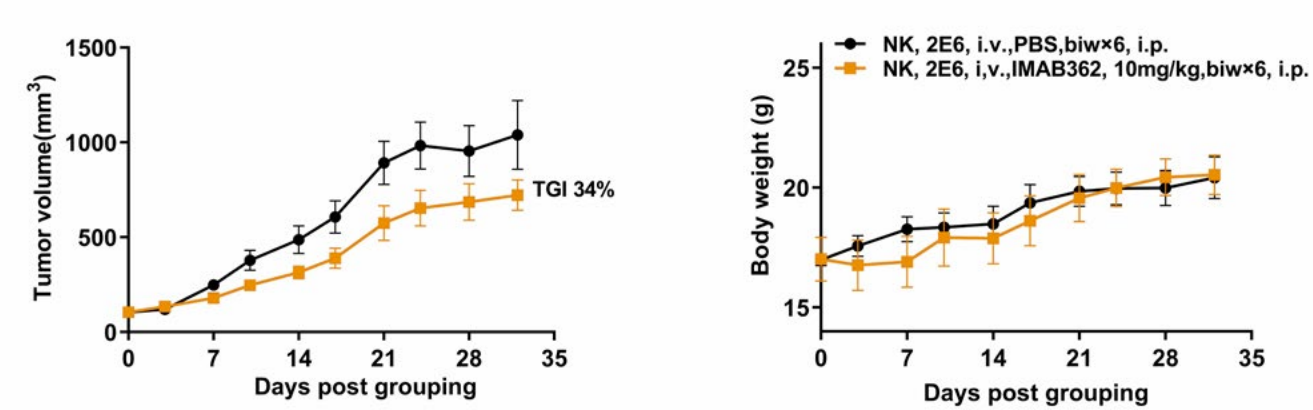

Immune cell phenotyping was conducted in the treated and untreated animals to assess any changes during the treatment study period. Flow cytometric analysis of peripheral blood showed that the proportions of human CD45, CD56, CD16, and NK T cells in the IMAB362 treated group was higher than that of the untreated control group (Figure 20), indicating that high levels of NK cells were maintained throughout the study period.

Figure 20: Human immune cell phenotyping of IMAB362 treated and untreated B-NDG hIL15 animals implanted with A549-hCLDN18.2 cells.

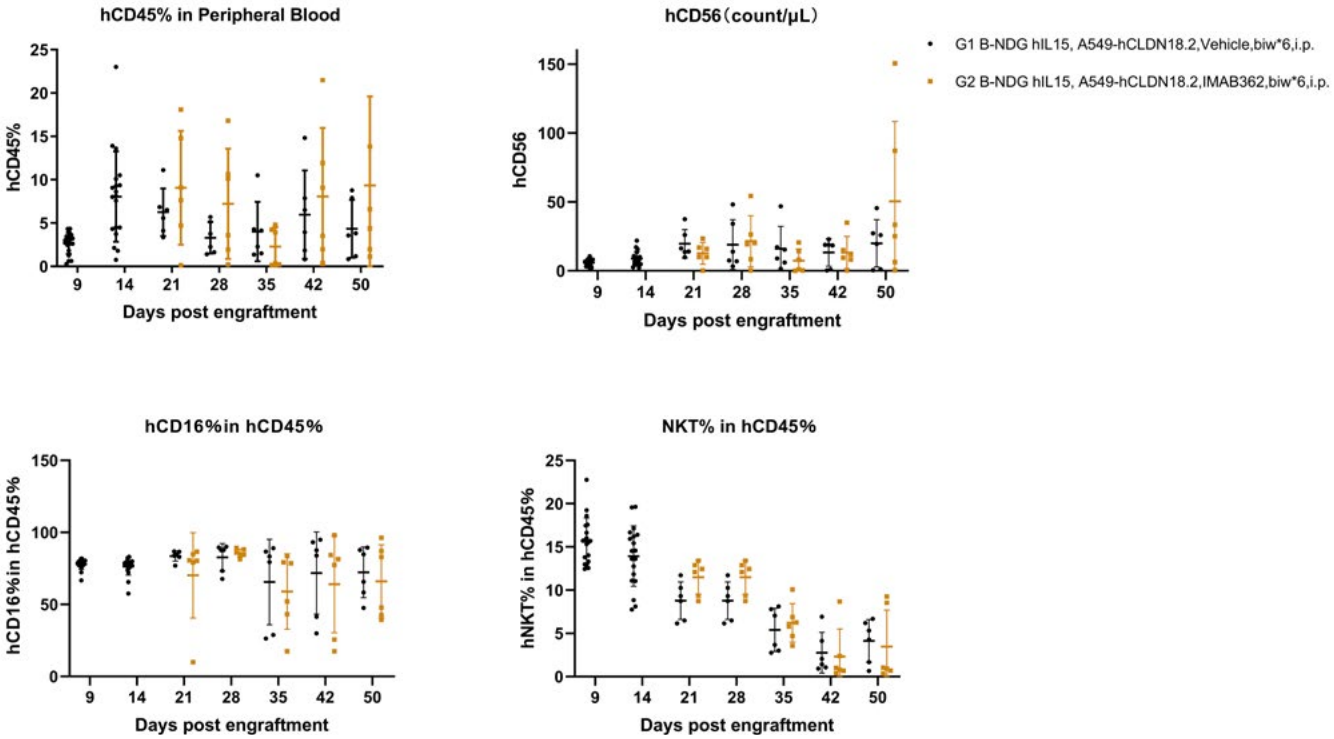

Summary

The novel B-NDG hIL15 strain combines the immunodeficient B-NDG mouse with expression of the human IL15 cytokine, which is essential for establishing NK cells. Expression of hIL15 boosts the development and survival of functional human NK cells in the context of immunodeficient mice engrafted with human cells. This novel model is especially valuable for evaluating immunotherapies targeting NK cells and their function in tumorigenesis.

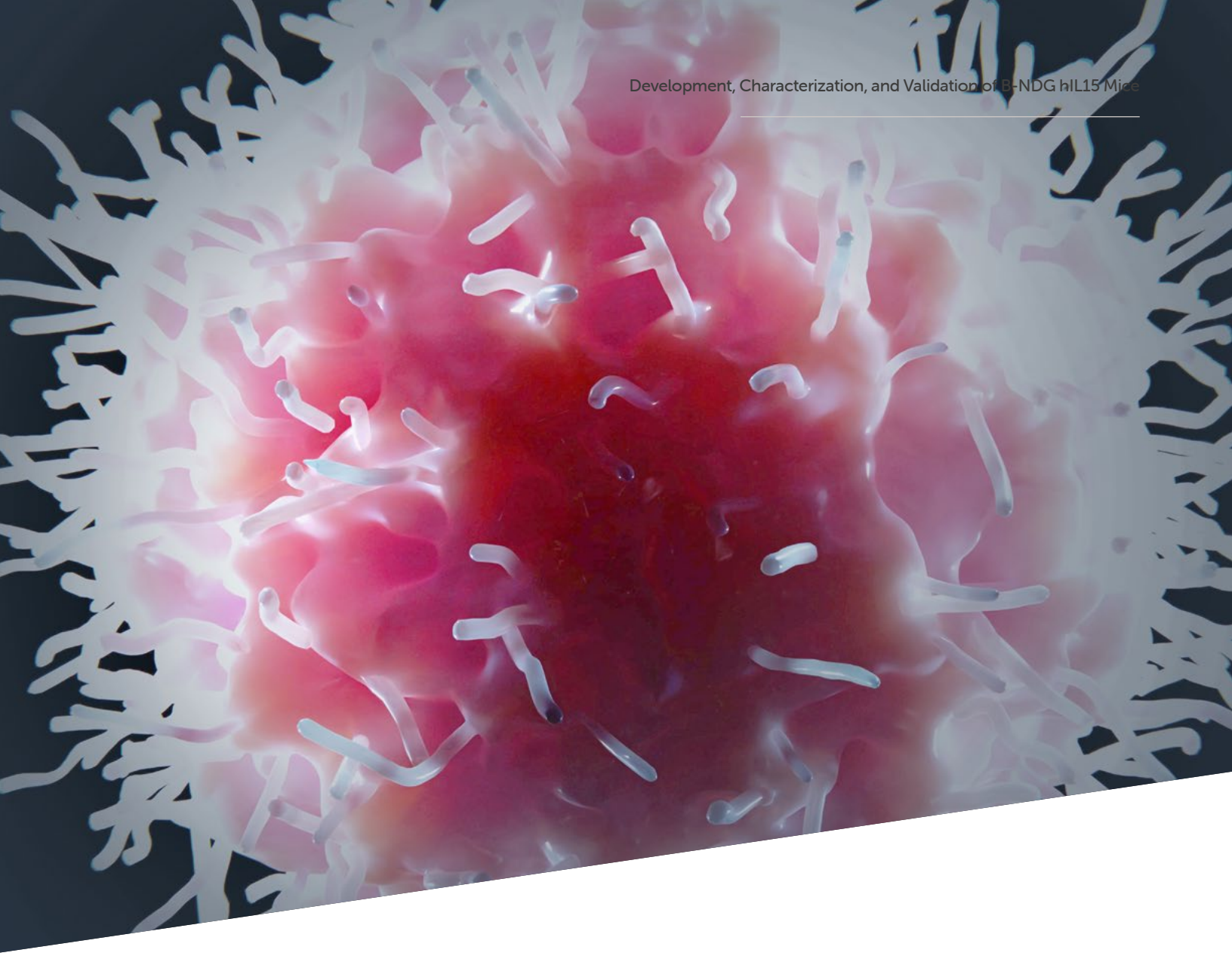

References

1. Cooper MA, Bush JE, Fehniger TA, VanDeusen JB, Waite RE, Liu Y, Aguila HL, Caligiuri MA. In vivo evidence for a dependence on interleukin 15 for survival of natural killer cells. Blood. 2002 Nov 15;100(10):3633-8.
2. Lin Q, Hu Y, Zhou X, Su Y, Shen Y. Long-term maintenance of human mature NK cells from hCD34+ HSCs engraftment supported by immune humanized B-NDG hIL15 mice [abstract]. In: Proceedings of the Annual Meeting of the American Association for Cancer Research 2020; Apr 27-28 and Jun 22-24. Philadelphia (PA): AACR; Cancer Res 2020;80(16 Suppl):Abstract nr 1632.
3. Kennedy MK, Glaccum M, Brown SN, Butz EA, Viney JL, Embers M, Matsuki N, Charrier K, Sedger L, Willis CR, Brasel K, Morrissey PJ, Stocking K, Schuh JC, Joyce S, Peschon JJ. Reversible defects in natural killer and memory CD8 T cell lineages in interleukin 15-deficient mice. J Exp Med. 2000 Mar 6;191(5):771-80.
4. Meza Guzman LG, Keating N, Nicholson SE. Natural Killer Cells: Tumor Surveillance and Signaling. Cancers (Basel). 2020 Apr 11;12(4):952.
5. Rudnicka D, Oszmiana A, Finch DK, Strickland I, Schofield DJ, Lowe DC, Sleeman MA, Davis DM. Rituximab causes a polarization of B cells that augments its therapeutic function in NK-cell-mediated antibody-dependent cellular cytotoxicity. Blood. 2013 Jun 6;121(23):4694-702.
6. Solomon BL, Garrido-Laguna I. TIGIT: a novel immunotherapy target moving from bench to bedside. Cancer Immunol Immunother. 2018 Nov;67(11):1659-1667. doi: 10.1007/s00262-018-2246-5.
7. Wu SY, Fu T, Jiang YZ, Shao ZM. Natural killer cells in cancer biology and therapy. Molecular cancer. 2020 Dec;19(1):1-26.
8. Wu Y, Tian Z, Wei H. Developmental and Functional Control of Natural Killer Cells by Cytokines. Front Immunol. 2017 Aug 4;8:930.

inōtiv

analyze. answer. advance.

Get in touch for a free consultation to support you in the maintenance of healthy animal populations critical to research integrity.

Visit **inotivco.com**